Mon. Not. R. Astron. Soc. **000**, 1–5 () Printed 16 December 2013 (MN LaTeX style file v2.2)

Ancient giants: on the farthest galaxy at $z = 8.6$

Pratika Dayal[1,2⋆], & Andrea Ferrara[3]
[1] *Leibniz Institute for Astrophysics, An der Sternwarte 16, Potsdam, Germany, 14482*
[2]

2

2 THEORETICAL MODEL

We start from the analysis of a $z = 8.6$ snapshot of a set of cosmological simulations carried out using the TreePM-SPH code GADGET-2 (Springel 2005) with the implementation of chemodynamics as described in Tornatore et al. (2007). The periodic simulation box has a comoving size of $75h^{-1}$Mpc and initially contains 512^3 particles each of dark matter (DM) and gas. The masses of the DM and gas particles are $m_{\rm DM}$ $1.7 \times 10^8\, h^{-1}{\rm M}_\odot$ and $m_{\rm gas}$ $4.1 \times 10^7\, h^{-1}{\rm M}_\odot$, respectively. For each "bona-fide" galaxy (which has at least 20 bound particles; see Saro et al. 2006 for details) in the simulated volume at $z = 8.6$, we compute the DM halo/stellar/gas mass, star formation rate (SFR), mass-weighted age, gas/stellar metallicity, and gas temperature. The adopted cosmological model for this work corresponds to the ΛCDM Universe with $\Omega_{\rm m} = 0.26, \Omega_\Lambda = 0.74$, $\Omega_{\rm b} = 0.0413$, $n_s = 0.95$, $H_0 = (100h) = 73$ km s^{-1} Mpc^{-1} and $\sigma_8 = 0.8$, thus consistent with the 5-year analysis of the WMAP data (Komatsu et al. 2009). Complete details of these simulation runs can be found in Dayal et al. (2009).

2.1 Intrinsic luminosities and dust

Star forming galaxies produce their intrinsic Lyα line and UV continuum luminosities (L_α^{int} and L_c^{int}, at restframe wavelengths $\lambda_\alpha = 1216$ Å and $\lambda_c = 1700$ Å, respectively) both via stellar (and nebular) emission, and cooling radiation from collisionally excited neutral hydrogen (H I) in their interstellar medium (ISM). While the spectral energy distributions (SEDs) are obtained using the population synthesis code STARBURST99 (Leitherer et al. 1999) to calculate the stellar and nebular emission, the latter depends on the temperature distribution in the ISM gas. The interested reader is referred to previous work (Dayal, Ferrara & Saro 2010) for a comprehensive discussion.

As Lyα and continuum photons are efficiently absorbed by dust grains, we calculate the dust content of each galaxy by considering SNII to be the main dust producers; this is justified by the fact that the typical evolutionary timescale of evolved stars ($\geqslant 1$ Gyr) becomes longer than the age of the Universe above $z \gtrsim 5.7$ (Todini & Ferrara 2001). We further pose that: (i) $0.5\,{\rm M}_\odot$ of dust is produced per SNII (Todini & Ferrara 2001; Nozawa et al. 2007), (ii) SNII destroy dust in forward shocks with an efficiency of about 40% (McKee 1998; Seab & Shull 1983), and (iii) a homogeneous mixture of gas and dust is assimilated into further star formation. To calculate the dust optical depth, τ, to UV continuum photons, based on the results obtained at $z \sim 6.6$, we assume that dust is made up of carbonaceous grains and spatially distributed as the stars (Dayal, Ferrara & Saro 2010). The fraction of continuum photons escaping the galaxy undamped by dust is then $f_c = (1-e^{-\tau})\tau^{-1}$. The analogous quantity for Lyα photons is taken to be $f_\alpha = 1$ so as to obtain the *poss* Lyα luminosity emerging from the galaxy itself.

2.2 IGM transmission and source clustering

After escaping out of the galactic environment, Lyα photons are further attenuated as they travel through the IGM. Depending on the intergalactic hydrogen ionization state, only a fraction $0 < T_\alpha < 1$ of the Lyα photons emerging out of a galaxy undamped by dust reaches the observer (continuum photons are instead unaffected by the IGM); T_α hence depends upon the IGM ionization state. Since this value is largely unconstrained, we explore 6 different values of the average IGM H I fraction at $z = 8.6$: $\chi_{HI} = 0.2, 0.3, 0.4, 0.5, 0.6, 0.7$. For each value of χ_{HI}, we compute the nominal radius, R_I, of the spherical, ionized HII region around each simulated galaxy. In reality, though, due to source clustering (i.e. when the separation between any two galaxies becomes smaller than either of their ionized region radii), multiple galaxies can contribute ionizing photons to the same ionized region, which will then be characterized by an radius, $R_I^{eff} > R_I$, calculated as follows. Suppose galaxies 'A' and 'B', and 'B' and 'C' have overlapping ionized regions. Then, the effective ionized volume 'A' is embedded in is the sum of the ionized volumes of 'A', 'B' and 'C'; the same holds true for both 'B' and 'C'. Within this ionized volume, the total photoionization rate at distance r from 'A', is

$$\Gamma^A_{tot}(r) \quad \int_{\nu_L}^{\infty} \frac{L^{em}_{\nu,A}}{4\pi r^2} \frac{\sigma_L}{h\nu} \left(\frac{\nu_L}{\nu}\right)^3 d\nu + \sum_{i=1, i\neq A}^{N} \int_{\nu_L}^{\infty} \frac{L^{em}_{\nu,i}}{4\pi r^2_{iA}} \frac{\sigma_L}{h\nu} \left(\frac{\nu_L}{\nu}\right)^3 d\nu + \Gamma_B,$$

where the terms on the right hand side represent the photoionization rate from (i) the direct radiation from 'A', (ii) the galaxies clustered around 'A' and (iii) the ultraviolet background (UVB) from distant galaxies, respectively. The UVB photoionization rate is related to χ_{HI} by $\Gamma_B = (1-\chi_{HI})^2 \chi_{HI}^{-1} n_H \alpha_B$ where n_H is the mean IGM hydrogen number density and α_B is the case-B hydrogen recombination coefficient. Further, $L^{em}_{\nu,A} = L^{int}_\nu f_{esc}$, is the specific ionizing luminosity emerging from 'A' and $f_{esc} = 0.02$ is the escape fraction of H I ionizing photons (Gnedin et al. 2008), $L^{em}_{\nu,i}$ is the ionizing luminosity emerging from the i^{th} galaxy of the total 'N' galaxies with which 'A' shares an ionized region, ν_L is the frequency corresponding to the Lyman limit wavelength (912 Å), σ_L is the hydrogen photoionization cross-section and r_{iA} is the distance between galaxies i and 'A'. This procedure is carried out for each galaxy in the simulated volume. We then assume photoionization equilibrium to compute χ_{HI} within the effective ionized region of each galaxy. At the edge of this region, we force χ_{HI} to attain the assigned global value. We use the complete Voigt profile to calculate the optical depth of Lyα photons along the line of sight to compute T_α. The observed Lyα and UV continuum luminosity are then simply $L_\alpha = L_\alpha^{int} f_\alpha T_\alpha = L_\alpha^{int} T_\alpha$ (the latter equality descends from our maximal assumption $f_\alpha = 1$), and $L_c = L_c^{int} f_c$, respectively.

As a final step, we select galaxies that would be observable as LAEs according to the canonical criterion, $L_\alpha \geqslant 10^{42.2}\,{\rm erg\,s^{-1}}$ *n* observed equivalent width $EW \geqslant 20$ Å. Among these, we further isolate those that fall within the L_α and continuum magnitude M_{UV} range observed by Lehnert et al. (2010) and Finkelstein et al. (2010): using SINFONI, the former find $L_\alpha = (2.7-8.3) \times 10^{42}\,{\rm erg\,s^{-1}}$, $M_{UV} = -19.6$ to -18.6, while Finkelstein et al. (2010) find a tighter bound of $M_{UV} = -19.2$ to -19.0. To summarize, all simulated galaxies that have $L_\alpha = (2.7-8.3) \times 10^{42}\,{\rm erg\,s^{-1}}$

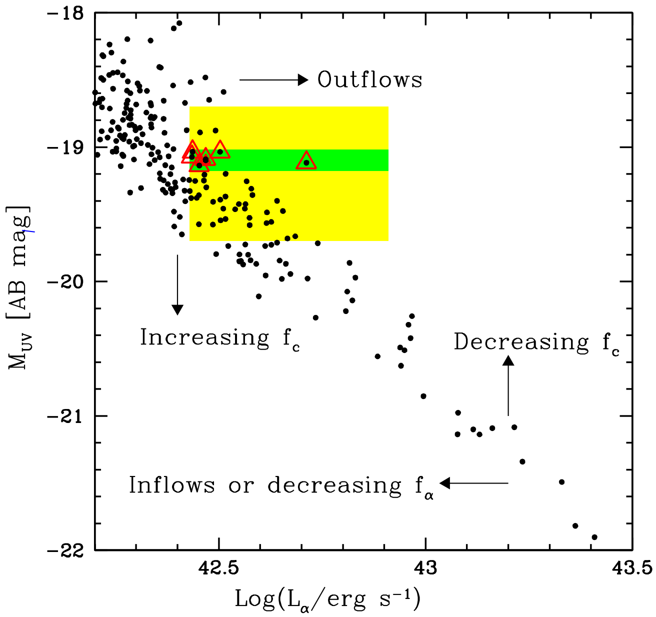

Figure 1. The UV magnitude plotted as a function of the observed Lyα luminosity for LAEs at $z = 8.6$. The yellow shaded area delimitates the region of the parameters deduced from the observation of UDFy-38135539 by Lehnert et al. (2010), the green shaded area shows the UV magnitude range measured for the same galaxy by Finkelstein et al. (2010) and points represent galaxies identified as LAEs in our simulation; the 7 LAE$_{UDF}$ for $\chi_{HI} = 0.2$ are marked by triangles. Arrows show the effects of different physical processes on the observed luminosity (see text for details).

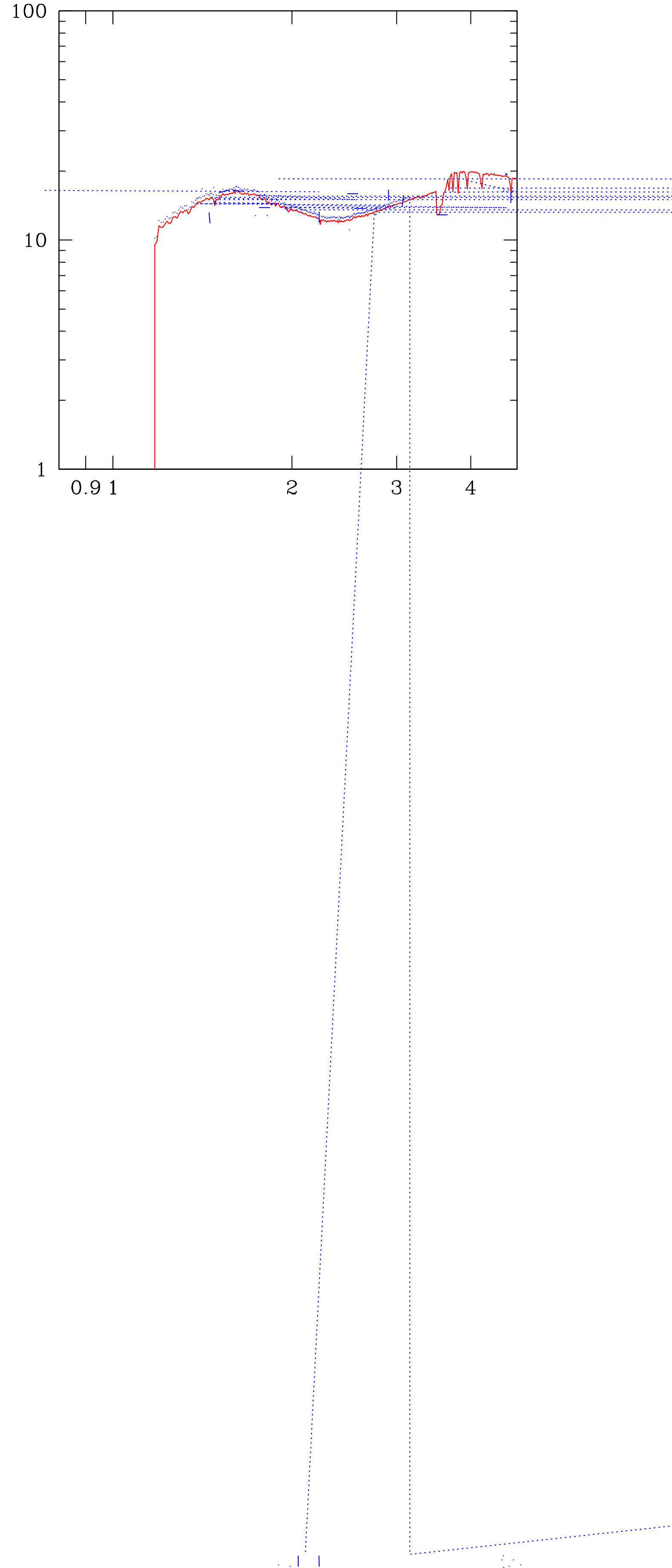

and $M_{UV} = -19.2$ to -19.0 and designated as LAE$_{UDF}$ in this work.

3 RESULTS

We now discuss the main results obtained from the above mentioned computations. We find that, without requiring any tuning of the model parameters, *no* LAE$_{UDF}$ are found in the simulated volume for $\chi_{HI} > 0.2$. For $\chi_{HI} = 0.2$, we find a total of 215 LAEs in the simulated volume, 7 of which are identified as LAE$_{UDF}$ as shown in Fig. 1. From now on, LAE$_{UDF}$ refer to the LAEs in the combined observed Lyα and UV luminosity range of Lehnert et al. (2010) and Finkelstein et al. (2010) for $\chi_{HI} = 0.2$.

We digress here to discuss the two main ingredients whose combined effects can change the slope of the $L_\alpha - M_{UV}$ relation shown in Fig. 1. The first of these concerns the dust attenuation: for any given LAE, an increase (decrease) in f_c leads to the galaxy becoming brighter (fainter) in the UV, shifting the position of the galaxy vertically upward (downward) on the plot; a decrease in the value of f_α (recall that we have used $f_\alpha = 1$ in our model) due to dust attenuation of Lyα photons leads to a corresponding decrease in L_α, moving the points horizontally leftward on the plot. The second effect is the change in T_α due to peculiar velocities: inflows (outflows) of neutral gas into (from) the galaxy impart an extra blueshift (redshift) to the Lyα photons, leading to a decrease (increase) in f_α (Santos 2004; Verhamme

[redacted]

volume by randomly placing the observed volume within it. We find that only 7 of these sub-volumes contain 1 LAE similar to UDFy-38135539 for $\chi_{HI} = 0.2$. This translates into a detection probability of only about 7%, classifying the discovery as a relatively serendipitous one.

4 CONCLUSIONS AND DISCUSSION

We have constrained the IGM ionization state at $z = 8.6$. We find that without requiring any fine-tuning of the model parameters from $z = 6.6$ and for the maximum possible Lyα luminosity emerging from the galaxy itself, *no* LAE are found in the observed luminosity range of UDFy-38135539 for $\chi_{HI} > 0.2$. For $\chi_{HI} = 0.2$, we find 7 LAEs (designated LAE$_{UDF}$) whose observed Lyα and UV luminosity fall in the ranges of UDFy-38135539 (Lehnert et al. 2010) and ID 125 (Finkelstein et al. 2010). LAE$_{UDF}$ are observable in the Lyα *on* because an overlapping of their H II regions with those of their nearby galaxies make the effective H II radius $\sim 0.24 - 0.42$ pMpc; averaged over the 7 LAE$_{UDF}$, there is a 70% (15%) probability of such a clustered source being found by JWST (HST/WFC3) observations.

We have also bracketed the physical properties of UDFy-38135539: the SFR range between $2.7 - 3.7\, M_\odot\,\mathrm{yr}^{-1}$, it has $10^{8.3-8.7} M_\odot$ of stars with a mass weighted age of 50-80 Myr and a mass weighted stellar metallicity between $0.03 - 0.12\, Z_\odot$. It is dust enriched with dust masses $\sim 10^{5.7-6} M_\odot$ which translates into $A_V \sim 0.75$ mag and a color excess of $E(B-V) \sim 0.16 - 0.19$ using the supernova dust extinction curve.

We add three caveats. The first concerns uncertainties related to dust attenuation of Lyα photons. As has been shown by many works (Neufeld 1991; Hansen & Oh 2006; Finkelstein et al. 2008; Dayal et al. 2009; Dayal, Ferrara & Saro 2010; Dayal, Maselli & Ferrara 2011), the relative escape fraction of Lyα and continuum photons depends on the distribution (smooth/clumpy) of dust in the ISM of high-z galaxies. Lacking data at $z \sim 8$ to support either of the two possibilities, here we have used the maximum value of $f_\alpha = 1$. Secondly, an increase (decrease) in the escape fraction of H I ionizing photons (f_{esc}) would decrease (increase) the intrinsic Lyα luminosity, while increasing (decreasing) the sizes of the H II regions built by each galaxy, thereby affecting the observed Lyα luminosity. Thirdly, outflows might allow Lyα photon transmission also from a substantially more neutral IGM (Dijkstra et al. 2011) than the upper limit of $\chi_{HI} > 0.2$ found here. Although interesting, such result has been obtained under the highly idealized conditions of a smooth, spherically symmetric expanding shell of HI gas, whose radius and column density have been tuned to suitable values. As it is very likely that shell fragmentation occurs as a result of Raleigh-Taylor and Kelvin-Helmholtz instabilities arising from the complex gas velocity field around the galaxy (e.g. see Fig. 2 of Fangano et al. 2007), such suggestion needs to await more detailed investigations.

5 ACKNOWLEDGEMENTS

PD acknowledges a Fellowship funded through the Marie Curie Early Stage Training project MEST-CT-2005-021074. PD thanks SISSA for their generous allocation of cluster time and the Scuola Normale Superiore for hospitality. We thank R. Salvaterra and the referee for insightful comments and M. Dijkstra for poitning out an error in an earlier version of the manuscript.

REFERENCES

Bianchi S., Schneider R., 2007, MNRAS, 378, 973
Bouwens R.J. et al., 2009, submitted to Nature, arXiv:0912.4263
XS
Dayal P., Ferrara A. & Gallerani S., 2008, MNRAS, 389, 1683
Dayal P., Ferrara A., Saro A., Salvaterra R., Borgani S., Tornatore L., 2009, MNRAS, 400, 2000
Dayal P., Ferrara A., Saro A., 2010, MNRAS, 402, 1449
Dayal P., Maselli A., Ferrara A., 2011, MNRAS, 410, 830
Dijkstra M., Wyithe S. J. B., 2010, MNRAS, 408, 352
Dijkstra M., Mesinger, A. Wyithe S. J. B., 2011, arXiv:1101.5160
Fangano, A. P. M., Ferrara, A., Richter, P. 2007, MNRAS, 381, 469
Finkelstein S.L., Rhoads J.E., Malhotra S., Grogin N., Wang J., 2008, ApJ, 678, 655
Finkelstein S.L., Papovich C., Giavalisco M., Reddy N. A., Ferguson H. C., Koekemoer A. M., Dickinson M., 2010, ApJ, 719, 1250
Giavalisco M. et al., 2004, ApJ, 600, 103
Gnedin N. Y., Kravtsov A. V., Chen, H.-W., 2008, ApJ, 672, 765
Hansen M., Oh S.P., 2006, MNRAS, 367, 979
Kashikawa N. et al., 2006, ApJ, 648, 7
Komatsu E. et. al., 2009, ApJS, 180, 330
Lehnert M. D. et. al., 2010, Nature, 467, 940
Leitherer C. et al., 1999, ApJS, 123, 3
Madau P., Haardt F., Rees M. J., 1999, ApJ, 514, 648
Malhotra S. et al., 2005, ApJ, 626, 666
McKee C., 1989, Interstellar Dust: Proceedings of the 135th Symposium of the IAU. Symposium no. 135, Kluwer Academic Publishers, Dordrecht, p. 431
Neufeld D.A., 1991, ApJ, 370, 85
Nozawa T., Kozasa T., Habe A., Dwek E., Umeda H., Tominaga N., Maeda K., Nomoto K., 2007, ApJ, 666, 955
Santos M. R., 2004, MNRAS, 349, 1137
Salvaterra R. et al., 2009, Nature, 461, 1258
Saro A. et al., 2006, MNRAS, 373, 397
Seab C. G., Shull J. M., 1983, ApJ, 275, 652
Shimasaku K. et al., 2006, PASJ, 58, 313
Springel V., 2005, MNRAS, 364, 1105
Steidel C.C., Giavalisco M., Pettini M., Dickinson M., Adelberger K.L., 1996, ApJ, 462, L17
Tanvir N. et al., 2009, Nature, 461, 1254
Todini P., Ferrara A., 2001, MNRAS, 325, 726
Tornatore L., Borgani S., Dolag K., Matteucci F., 2007, MNRAS, 382, 1050
Vanzella E. et al., 2010, Preprint arXiv:1011.5500
Verhamme A., Schaerer D., Maselli A., 2006, A&A, 460, 397